

Supporting Information

A Covalent Organic Framework with 4 nm Open Pores

Mirjam Dogru, Andreas Sonnauer, Andrei Gavryushin, Paul Knochel and Thomas Bein*

Department of Chemistry and Center for NanoScience (CeNS), University of Munich,

Butenandtstr. 5-13 (E), 81377 Munich, Germany,

Tel.: +49(0)89-2180-77623, Fax: +49(0)89-2180-77622, bein@lmu.de

1. Section: Materials and Methods

All materials (if not otherwise noted) were purchased from Aldrich or Fluka in the common purities purum and puriss. All materials were used without further purification. The building blocks 9,10-dimethyl-anthracene-2,3,6,7-tetraol (THDMA) and 1,3,5-benzenetris(4-phenylboronic acid) (BTPA) were prepared according to published procedures.^[1],^[1b] All materials were manipulated in air.

X-ray diffraction analysis was carried out in reflection mode using a Bruker D8 Discover with Ni-filtered CuK α -radiation (1.5406 Å) and a position-sensitive detector (Vantec). Fourier-transform infrared spectra of samples were measured with a Bruker Equinox 55 equipped with a PIKE MIRacle ATR-unit at room temperature. The SEM images were recorded with a Jeol 6500F field emission scanning electron microscope with an EDX/WDX detector. For this purpose the samples were put on an adhesive graphite film and sputtered with carbon with a BALTEC MED 020 Coating System. ¹¹B and ¹³C MAS NMR spectra were recorded on a Bruker DSX Avance 500 with a magnetic field of 11.2 Tesla. A 4 mm MAS triple-resonance sample head was used. The frequency of the rotor was 10 kHz. TG measurements were performed in a stream of synthetic air (25 ml / min) on a Netzsch STA 440 C TG/DSC. The measurements were carried out with a heating rate of 10 °C / min and a temperature range from 30 °C to 900 °C. The nitrogen sorption isotherms were recorded on a Nova 4000e at -196°C. Prior to the measurement of the adsorption isotherm the sample was treated as follows. The product was soaked in acetone for 2 days and heated for 24 h at 150°C under oil pump vacuum.

Molecular geometry optimization was performed with Accelrys MS Modeling 4.3 using the universal force field method. The final hexagonal unit cell was calculated with the geometrical parameters from the optimized structure. For the simulation of the PXRD pattern Reflex was used (a software package implemented in MS Modeling 4.3). For this purpose the unit cell parameters were first calculated and then refined from the experimentally observed peak positions in a hexagonal array. As a result we obtained cell parameters of $a = b = 43.65$ Å and $c = 3.52$ Å. The simulated PXRD patterns were then compared with the experimentally obtained data. We note that this structure can assemble in two different arrangements, i.e., (i) a staggered AB type with graphite-like packing, and (ii) an eclipsed AA type arrangement with the adjacent sheets lying exactly on top of each other. After optimizing the geometry of each arrangement, the powder patterns were simulated and compared to the experimental patterns. The simulated pattern of the AA arrangement shows very good agreement with our experimental PXRD pattern.

2. Synthesis

Synthesis optimization with high throughput methods

High throughput methods allowed us to find the optimal reaction conditions for the BTP-COF formation in a fast and efficient manner. In Table S1 we present the list of different solvent mixtures and stoichiometric ratios. Successful network formation was only observed with the highlighted solvents anisole and methanol at a ratio 90 to 10. The other solvent mixtures resulted in amorphous material.

Table S1 Overview of solvents and solvent ratios investigated for the formation of BTP-COF.

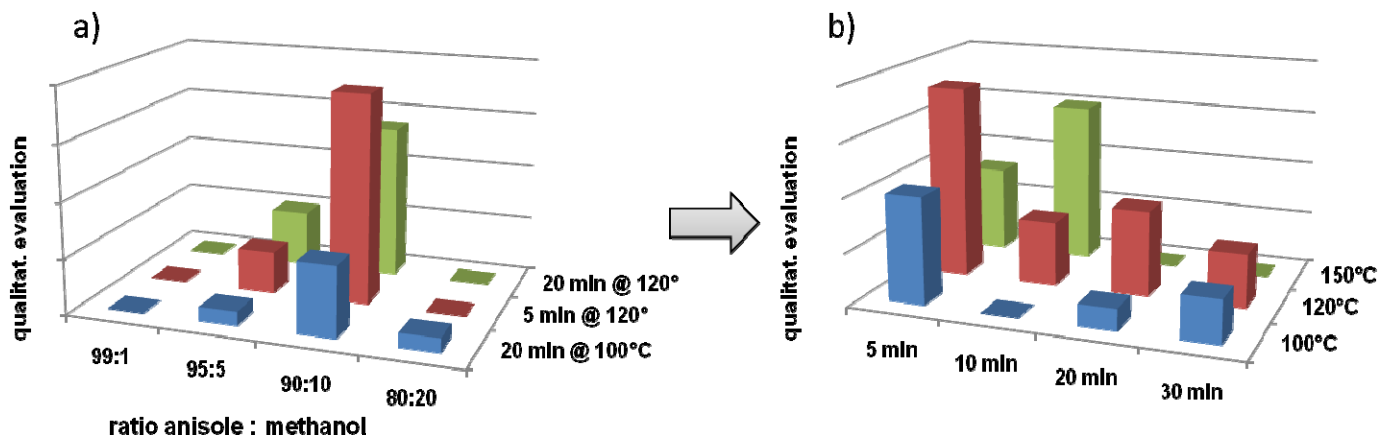
Solvent	Solvent	ratio
Mesitylene	Dioxane	50 : 50
Mesitylene	Methanol	99 : 1 / 98 : 2 / 95 : 5 / 90 : 10
Mesitylene	Acetone	99 : 1 / 98 : 2 / 95 : 5 / 90 : 10
Anisole	Dioxane	50 : 50
Anisole	Methanol	99 : 1 / 98 : 2 / 95 : 5 / 90 : 10 / 80 : 20
Anisole	Acetone	99 : 1 / 98 : 2 / 95 : 5 / 90 : 10
Toluene	Dioxane	50 : 50
Toluene	Methanol	99 : 1 / 98 : 2 / 95 : 5 / 90 : 10
THF	Dioxane	50 : 50
THF	Methanol	99 : 1 / 98 : 2 / 95 : 5 / 90 : 10

The framework only forms with anisole and methanol as solvents; with this knowledge the next steps were to improve crystallinity and yield of the product. Therefore, in the following experiments the ratio of the starting materials (0.1mmol BTPA to 0.2 mmol DMTHA) and the solvent mixture anisole to methanol at the ratio 90:10 were kept constant and reaction time, temperature and concentration were varied (see Table S2).

Table S2 Overview of volumes, reaction times and reaction temperatures investigated for BTP-COF.

Solvents	Volume (ml)	Time (min)	Temperature (°C)
Anisole:MeOH 90 : 10	1.0 to 2.7 ml / 0.2 steps	5 to 30 min / 5°C steps 45 min and 60 min	80°C to 120°C / 20°C 150°C and 170°C

Results of these experiments were evaluated and depicted in the semi-quantitative Scheme S1.



Scheme S1: Semi-quantitative evaluation of the synthesis optimization; evaluation based on comparable crystallinity and yield of the products.

Optimized synthesis parameters

Following optimization in a high-throughput screening approach, the following recipe was established for the synthesis of the new BTP-COF. In a 5 ml Biotage microwave vial the solid mixture of 0.1 mmol (43 mg) 1,3,5-benzentrif(4-phenylboronic) acid **BTPA** and 0.2 mmol (63 mg) 9,10-dimethyl-anthracene-2,3,6,7-tetraol **THDMA** was dissolved in 1.5 ml anisole and methanol (9:1 v:v). The cloudy solution in the tightly capped vial was heated to 120°C for 5 min in the Biotage microwave Initiator 2.0. The resulting green powder was isolated by filtration and excessive washing with 50 ml dry acetone (Aldrich). The powder was dried at room temperature, yielding 72% (53 mg) based on BTPA. For gas adsorption measurements the product was soaked in acetone for 2 d and heated at 150 °C under dynamic vacuum for 24 h.

FT-ATR-IR: ν (cm⁻¹) = 3493 (m), 2977 (w), 1605 (m), 1495 (m), 1457 (m), 1386 (m), 1356 (s), 1247 (m), 1210 (s), 1063 (m), 1042 (w), 1016 (m), 889 (m), 822 (m), 755 (m).

3. Structural Models and X-ray Analyses

Table 1: Refined crystal data

Formula	C ₉₆ H ₆₀ B ₆ O ₁₂
Formula Weight	1470.39
Crystal system	Hexagonal
Space group	P6/mmm
Unit cell dimensions	a = b = 43.65 Å c = 3.52 Å
Cell Volume	5808.20 Å ³

Table 2: Fractional atomic coordinates

Atom	Wyck.	x	y	z
C1	6k	0.56448	0.56448	0.50
C2	6k	0.5313	0.5313	0.50
O3	12q	0.40998	0.53542	0.50
C4	12q	0.43782	0.53067	0.50
C5	12q	0.46856	0.4998	0.50
C6	12q	0.43727	0.49988	0.50
C7	12q	0.3539	0.59285	0.50

C8	12q	0.37178	0.57515	0.50
B12	6m	0.42719	0.57281	0.50
C13	6m	0.40729	0.59271	0.50
C14	6m	0.35155	0.64845	0.50
C15	6m	0.37099	0.62901	0.50
C16	6m	0.31564	0.63127	0.50

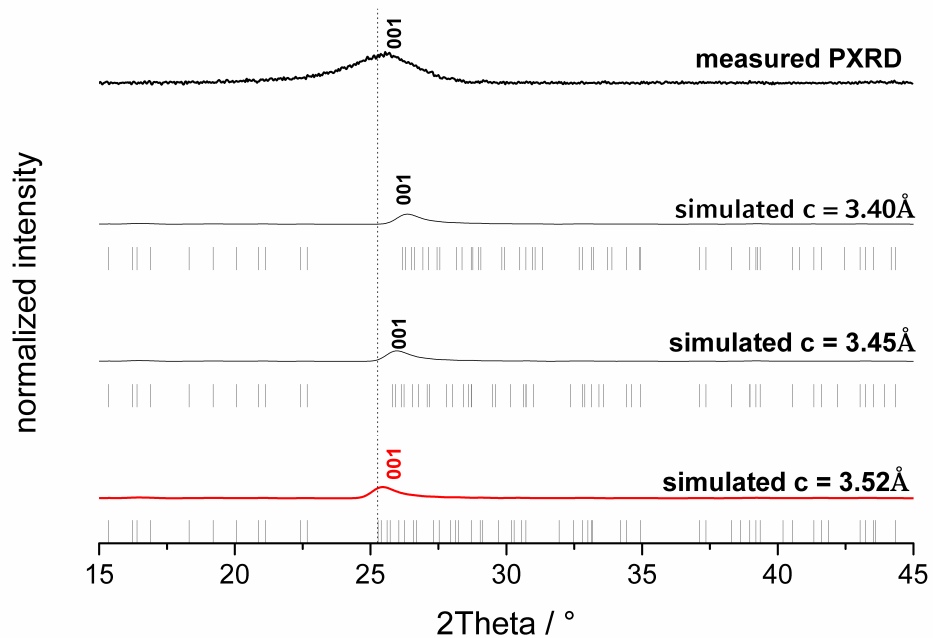


Figure S1: Comparison of the 001 reflection of measured PXRD with simulated patterns having different interlayer distances. Best fit was obtained for a distance of 3.52 Å.

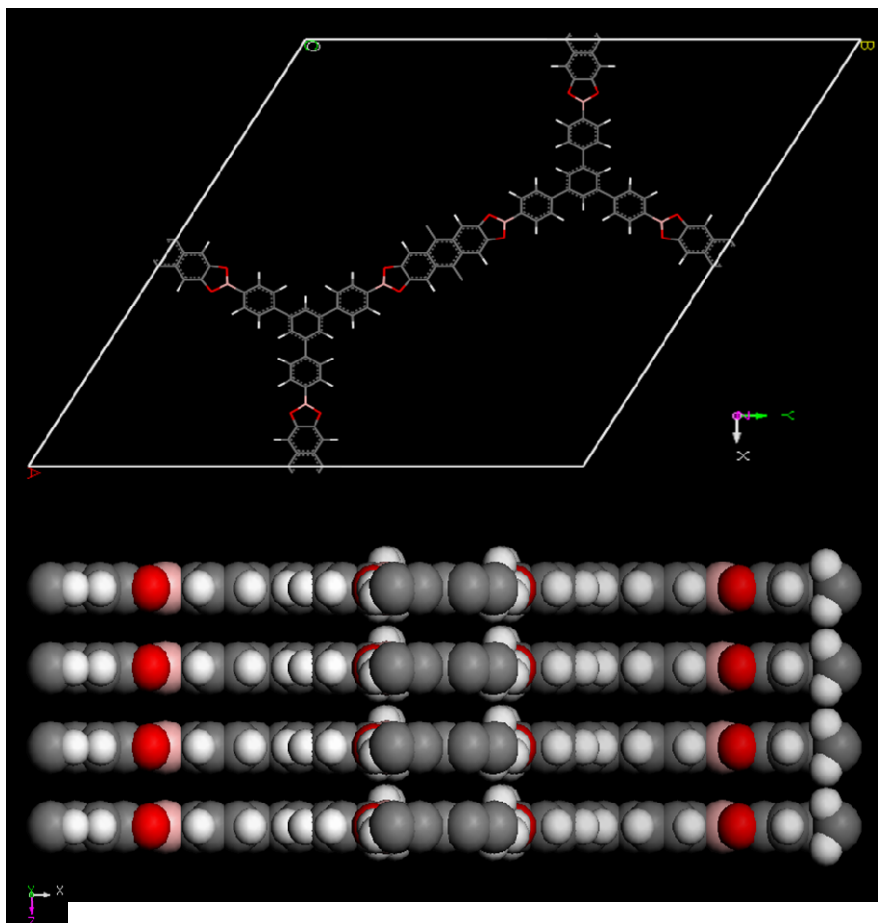


Figure S2: Simulation of crystal lattice of the unit cell calculated in an eclipsed arrangement: a) top view in AB plane, b) view along c-axis with slightly larger interlayer distance due to the rotating methyl groups.

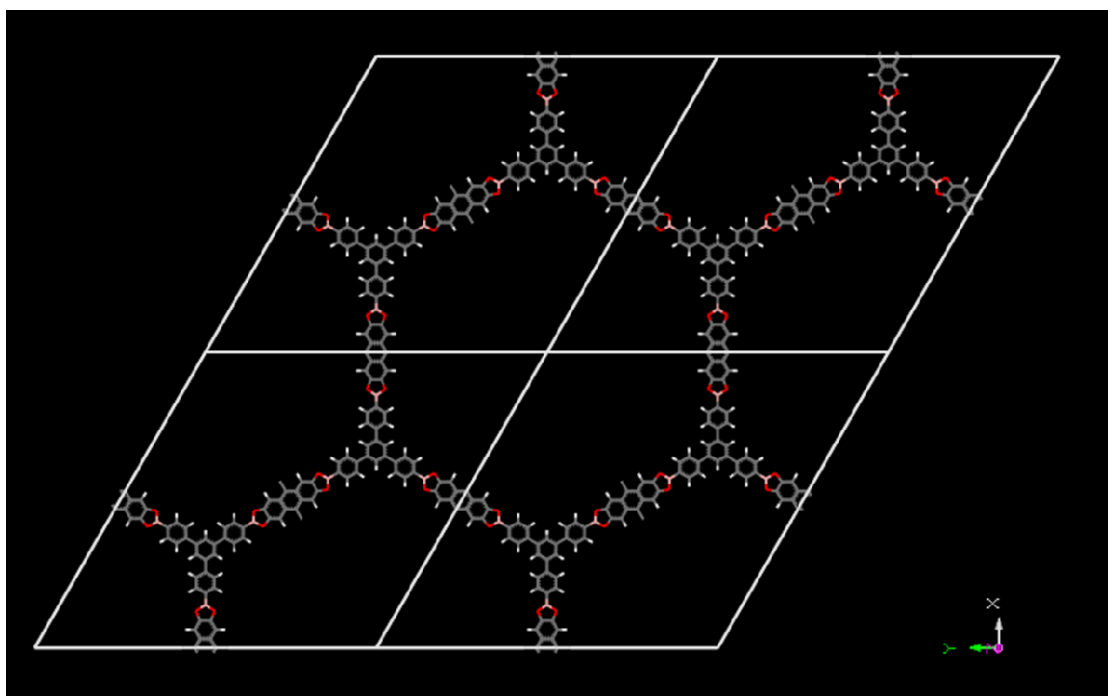


Figure S3: Crystal structure of four unit cells in AB plane of the eclipsed arrangement.

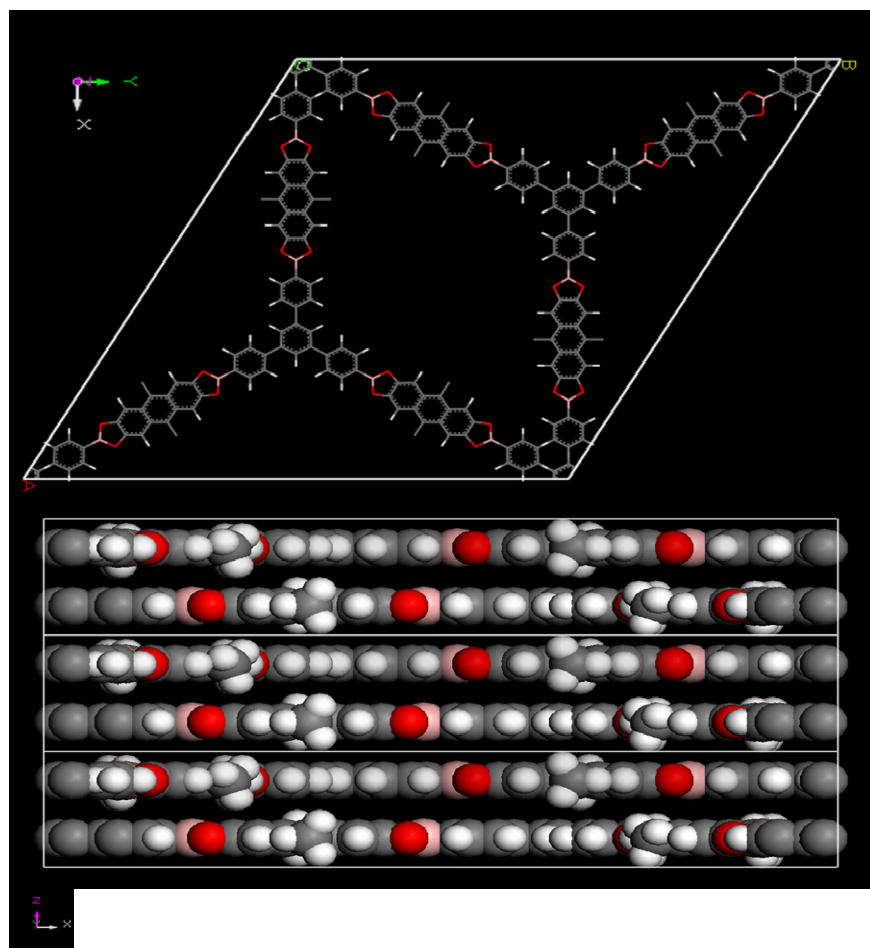


Figure S4: Simulation of crystal lattice of the unit cell calculated in a staggered arrangement (space group $P6_3/mmc$): a) top view in AB plane, it is obvious that the pore size and hence the internal surface is significantly smaller than the experimental data. b) View along c-axis with larger interlayer distance due to doubling of the sheets, this would lead to a much smaller 2θ value for the 001 reflex than the experimentally obtained one.

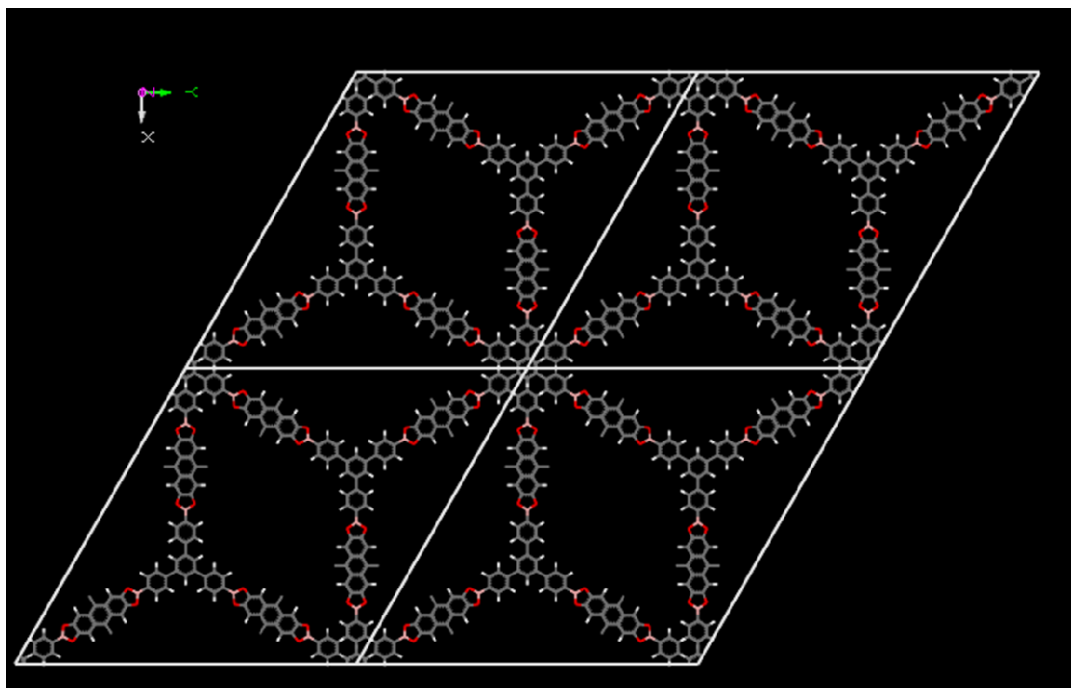


Figure S5: Crystal structure of four unit cells in AB plane of the staggered arrangement.

4. Scanning Electron Microscopy imaging (SEM)

The SEM images of the material show very small crystals of about 100 nm. However, these values are quite large compared to the values calculated from the peak broadening of the powder pattern. This leads to the conclusion that intergrowth of small domains occurs. The SEM image also shows the jagged morphology of the material.

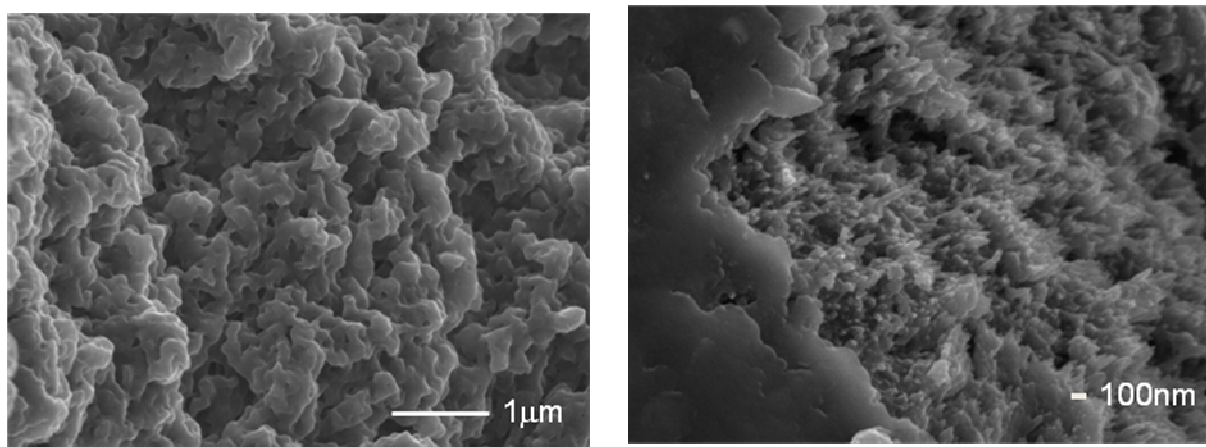


Figure S6: SEM micrographs of the BTP-COF.

5. FT-IR Microscopy

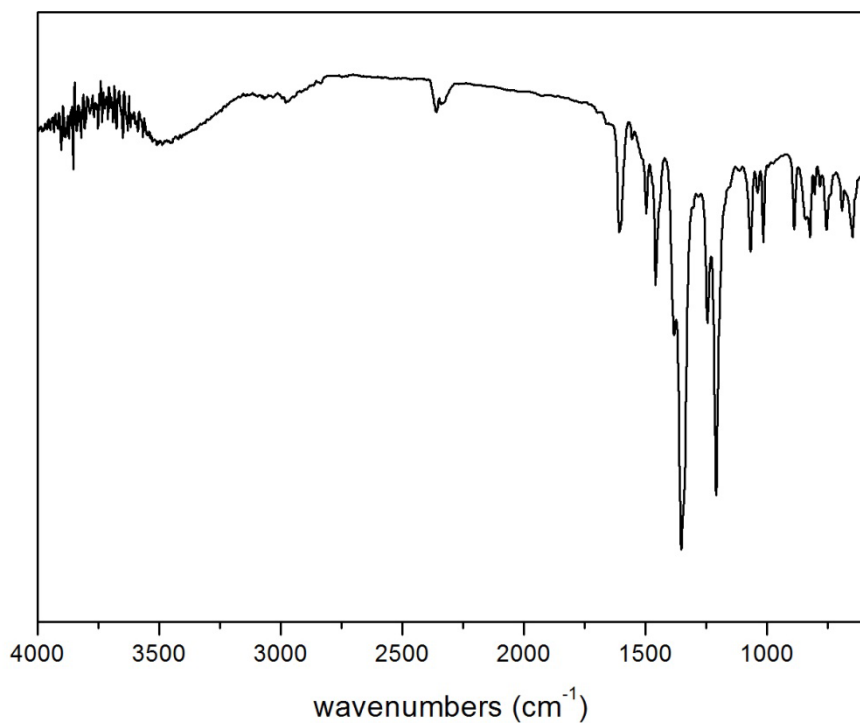


Figure S7: FT-IR spectrum of the BTP-COF with 4 nm pores.

Table 3: Assignment of the most important peaks in the infrared spectrum of the BTP-COF

Peak (cm^{-1})	Assignment
3495 (m)	ν_{sym} OH from terminal OH and $\text{B}(\text{OH})_2$ groups
2977(w)	ν_{asym} Ar-CH ₃
2837(w)	Ar-C-H ₃
1606(m)	ν_{sym} C=C for fused aromatics
1496(m)	ν_{sym} C=C for aromatics
1458(m)	ν_{sym} C=C for aromatics
1382(s)	ν_{sym} B-O
1352(s)	ν_{sym} B-O
1245(m)	ν_{sym} C-O
1207(s)	C-H in plane bending for p-substituted benzene
1068(m)	
1039(w)	ν_{sym} B-C

6. ^{13}C CP-MAS Nuclear Magnetic Resonance

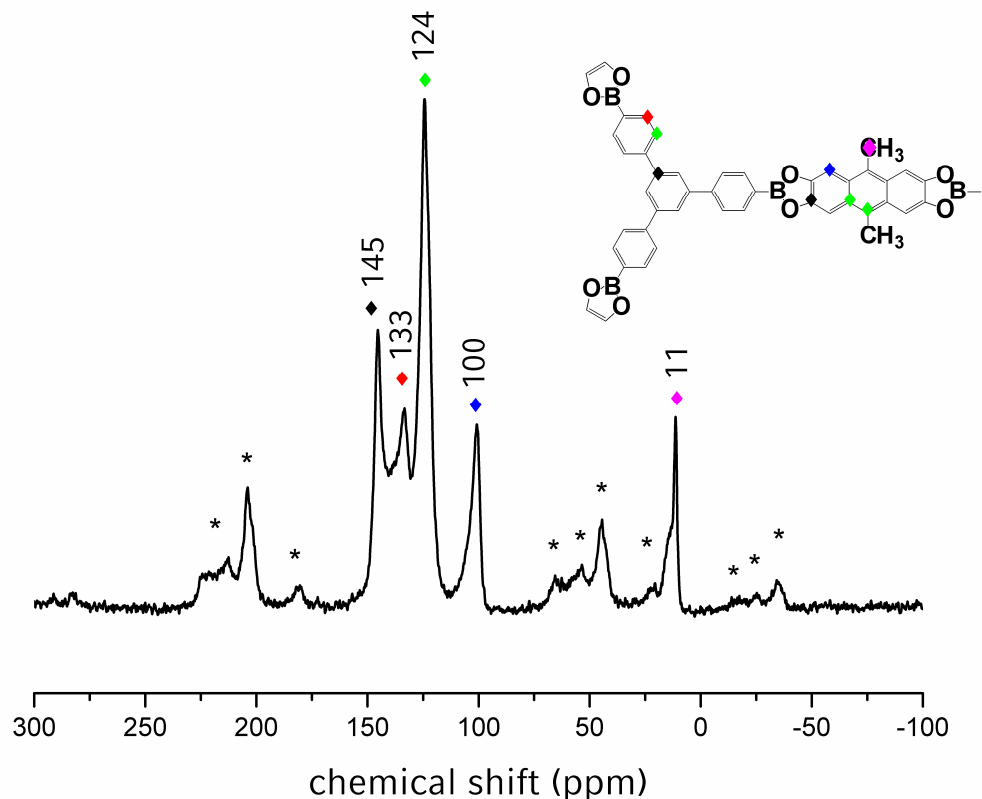


Figure S8: The ^{13}C CP-MAS NMR spectrum of BTP-COF indicates that the expected building blocks are present. Asterisks (*) indicate peaks arising from spinning side bands.

7. TGA

A first step with a weight loss of 11 % is observed between 50°C and 200°C. The next step with a weight loss of 61 % above 400 °C indicates the degradation of BTP-COF. At a temperature of 700 °C a total weight loss of 22% is reached, which corresponds to a quantity of B_2O_3 representing 6 boron atoms per unit cell (unit cell formula: $\text{C}_{96}\text{H}_{60}\text{B}_6\text{O}_{12}$).

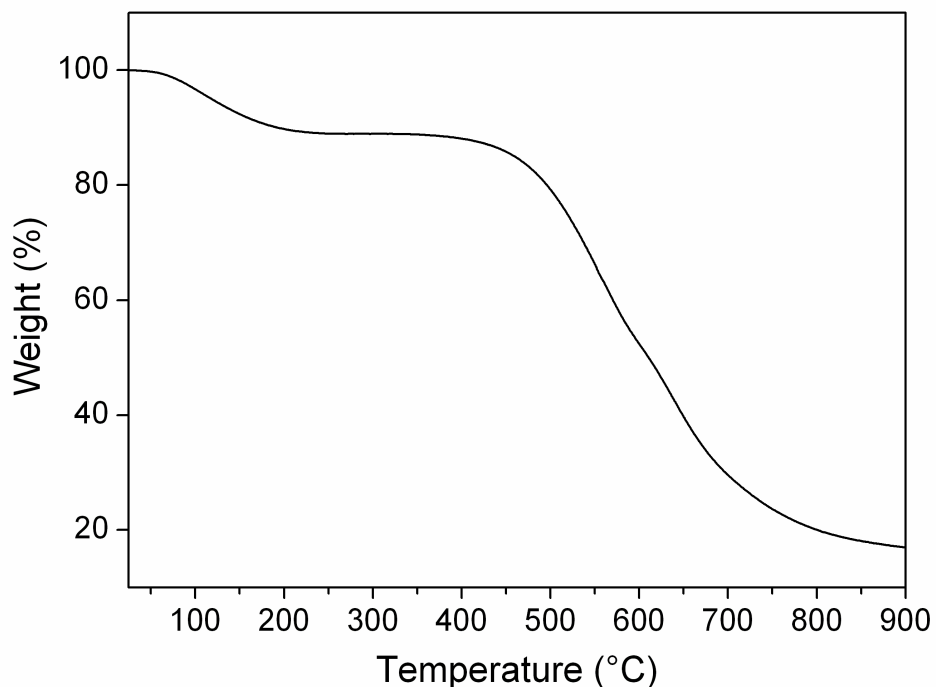


Figure S9: Thermogravimetric analysis of the BTP-COF.

- [1] a) Y. Chung, B. F. Duerr, T. A. McKelvey, P. Nanjappan, A. W. Czarnik, *The Journal of Organic Chemistry* **1989**, *54*, 1018; b) W.-H. Huang, W.-L. Jia, S. Wang, *Canadian Journal of Chemistry* **2006**, *84*, 477.